Available online at www.sciencedirect.com
SCIENCE DIRECT®
ELSEVIER
Nuclear Instruments and Methods in Physics Research A 516 (2004) 68–79
NUCLEAR INSTRUMENTS & METHODS IN PHYSICS RESEARCH
Section A
www.elsevier.com/locate/nima

Analysis of the liquid argon purity in the ICARUS T600 TPC

S. Amoruso[a], M. Antonello[b], P. Aprili[c], F. Arneodo[c], A. Badertscher[d], B. Baiboussinov[e], M. Baldo Ceolin[e], G. Battistoni[f], B. Bekman[g], P. Benetti[h], E. Bernardini[c], M. Bischofberger[d], A. Borio di Tigliole[h], R. Brunetti[h], R. Bruzzese[a], A. Bueno[d,i], M. Buzzanca[b], E. Calligarich[h], M. Campanelli[d], F. Carbonara[a], C. Carpanese[d], D. Cavalli[f], F. Cavanna[b], P. Cennini[j], S. Centro[e], A. Cesana[k], C. Chen[l], D. Chen[l], D.B. Chen[e], Y. Chen[l], X. Cieślik[m], D. Cline[n], A.G. Cocco[a], Z. Dai[d], C. De Vecchi[h], A. Dąbrowska[m], A. Di Cicco[a], R. Dolfini[h], A. Ereditato[a], M. Felcini[d], A. Ferrari[j,f], F. Ferri[b], G. Fiorillo[a], S. Galli[b], Y. Ge[d], D. Gibin[e], A. Gigli Berzolari[h], I. Gil-Botella[d], K. Graczyk[o], L. Grandi[h], A. Guglielmi[e], K. He[l], J. Holeczek[g], X. Huang[l], C. Juszczak[o], D. Kiełczewska[p,q], J. Kisiel[g], T. Kozłowski[q], M. Laffranchi[d], J. Łagoda[p], Z. Li[l], F. Lu[l], J. Ma[l], G. Mangano[a], M. Markiewicz[m], A. Martinez de la Ossa[i], C. Matthey[n], F. Mauri[h], G. Meng[e], M. Messina[d], C. Montanari[h], S. Muraro[f], S. Navas-Concha[d,i,*], G. Nurzia[b], S. Otwinowski[n], Q. Ouyang[l], O. Palamara[c], D. Pascoli[e], L. Periale[r,s], G.B. Piano Mortari[b], A. Piazzoli[h], P. Picchi[s,t,r], F. Pietropaolo[e], W. Półchłopek[u], T. Rancati[f], A. Rappoldi[h], G.L. Raselli[h], J. Rico[d], E. Rondio[q], M. Rossella[h], A. Rubbia[d], C. Rubbia[h], P. Sala[f,d], R. Santorelli[a], D. Scannicchio[h], E. Segreto[b], Y. Seo[n], F. Sergiampietri[v], J. Sobczyk[o], N. Spinelli[a], J. Stepaniak[q], M. Szarska[m], M. Szeptycka[q], M. Szleper[q], M. Terrani[k], R. Velotta[a], S. Ventura[e], C. Vignoli[h], H. Wang[n], X. Wang[a], J. Woo[n], G. Xu[l], Z. Xu[l], A. Zalewska[m], J. Zalipska[q], C. Zhang[l], Q. Zhang[l], S. Zhen[l], W. Zipper[g]

[a] *Università Federico II di Napoli e INFN, Napoli, Italy*
[b] *Università dell'Aquila e INFN, L'Aquila, Italy*
[c] *INFN - Laboratori Nazionali del Gran Sasso, Assergi, Italy*
[d] *Institute for Particle Physics, ETH Hönggerberg, Zürich, Switzerland*
[e] *Università di Padova e INFN, Padova, Italy*
[f] *Università di Milano e INFN, Milano, Italy*
[g] *Institute of Physics, University of Silesia, Katowice, Poland*
[h] *Università di Pavia e INFN, Pavia, Italy*
[i] *Depto de Física Teórica y del Cosmos & C.A.F.P.E., Universidad de Granada, Granada, Spain*
[j] *CERN, Geneva, Switzerland*

*Corresponding author. Address for correspondence: Depto de Física Teórica y del Cosmos & C.A.F.P.E., Campus de Fuente Nueva, Universidad de Granada, Granada E-18071, Spain. Tel.: +34-958-244152; fax: +34-958-248529.
E-mail addresses: navas@ugr.es (S. Navas-Concha).

doi:10.1016/j.nima.2003.07.043

[k] Politecnico di Milano (CESNEF), Milano, Italy
[l] IHEP—Academia Sinica, Beijing, People's Republic of China
[m] H.Niewodniczański Institute of Nuclear Physics, Kraków, Poland
[n] Department of Physics, UCLA, Los Angeles, CA, USA
[o] Institute of Theoretical Physics, Wrocław University, Wrocław, Poland
[p] Institute of Experimental Physics, Warsaw University, Warszawa, Poland
[q] A.Sołtan Institute for Nuclear Studies, Warszawa, Poland
[r] IFSI, Torino, Italy
[s] Università di Torino, Torino, Italy
[t] INFN Laboratori Nazionali di Frascati, Frascati, Italy
[u] AGH-University of Science and Technology, Kraków, Poland
[v] INFN, Pisa, Italy

ICARUS Collaboration

Received 17 July 2003; accepted 30 July 2003

Abstract

The results reported in this paper are based on the analysis of the data recorded with the first half-module of the ICARUS T600 liquid argon Time Projection Chamber (LAr TPC), during a technical run that took place on surface in Pavia (Italy). We include results from the linearity, uniformity and calibration of the electronics, measurements on the electron drift velocity in LAr at different electric fields, as well as the LAr purity achievement of the detector. Two complementary techniques were used to measure the drift electron lifetime inside the active volume: the first, from the data of a purity monitor, gives a measurement localized in space; the second, based on the study of the signals produced by long minimum ionizing tracks crossing the detector, provides a LAr volume averaged value. Both methods yield consistent results over the whole data taking period and are compatible with an uniform LAr purity over the whole volume. The maximal drift electron lifetime value was recorded before the run stop and was about 1.8 ms. From an interpretation of the observed drift electron lifetime as a function of time, we conclude that the adopted technology would allow for drift distances exceeding 3 m.

PACS: 29.40.Gx; 29.40.Vj; 29.85.+c; 29.90.+r

Keywords: Liquid argon; TPC; LAr purity; Electron drift velocity

1. Introduction

The ICARUS T600 liquid argon (LAr) detector [1] (see Fig. 1) consists of a large cryostat split in two identical, adjacent half-modules, each of $3.6 \times 3.9 \times 19.9\ \mathrm{m}^3$ internal dimensions. Each half-module is an independent unit housing an internal detector composed of two Time Projection Chambers (TPC), a field shaping system, monitors and probes, and of two arrays of photo-multipliers (PMTs). The cryostat is externally surrounded by a set of thermal insulation layers. The TPC wire read-out electronics is located on the top side of the cryostat. The detector layout is completed by a cryogenic plant made of a liquid nitrogen cooling circuit and of a system of LAr purifiers. More details on the ICARUS T600 can be found elsewhere [2].

A liquid argon TPC detecting the ionization charge released at the passage of charged particles in the volume of LAr, allows for three-dimensional image reconstruction and for calorimetric measurement of ionizing events. The detector, equipped with an electronic read-out system, works as an "electronic bubble chamber" employing LAr as ionization medium. Unlike traditional

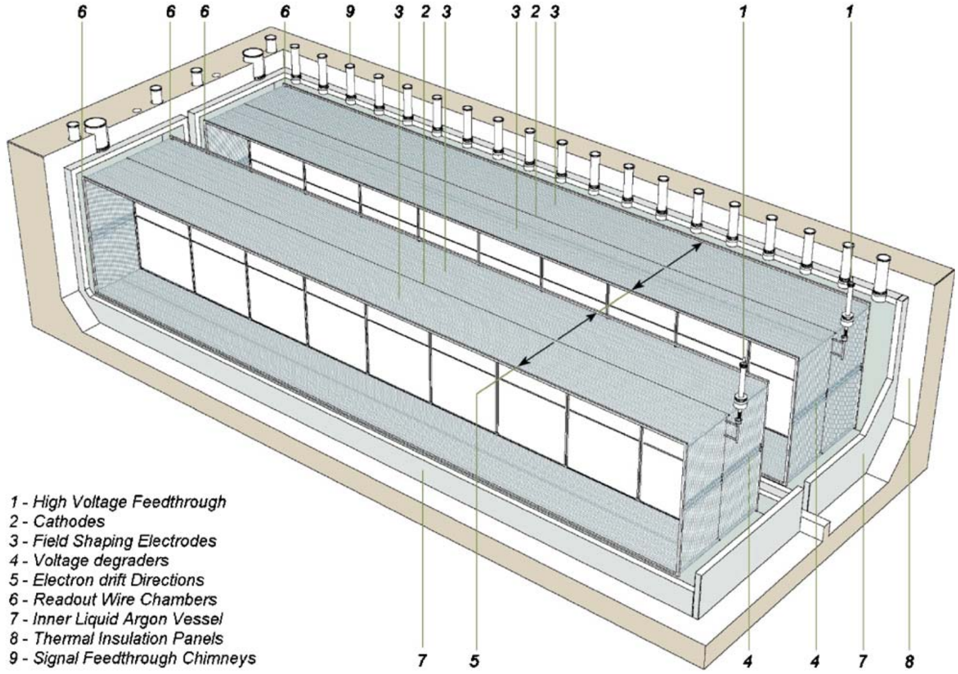

Fig. 1. Cut view of the ICARUS T600 module.

bubble chambers, limited by a short window of sensitivity after expansion, the LAr TPC detector remains fully and continuously sensitive, self-triggerable and without read-out dead time. The time when the ionizing event occurred (the so-called "T_0 time" of the event) can be determined by detection from the PMT arrays of the prompt scintillation light [3].

A uniform electric field applied to the medium makes the ionization electrons drift onto the anode, following the electric field lines; owing to the low transverse diffusion of the ionization charge, the electron images of ionizing tracks are preserved. Successive anode wire planes, biased at different potentials and oriented at different angles, make possible the three-dimensional reconstruction of the track image. While approaching a plane, the electrons induce a current on the wires near which they are drifting; when moving away after crossing the plane, a current of opposite sign is induced. By appropriate biasing, the first planes can be made non-destructive (*Induction* planes), whereas the charge is finally collected in the last plane (*Collection* plane). Each wire plane provides an independent view of the event.

In an ICARUS T600 half-module the two identical TPCs, referred to as *left* and *right* chambers, are separated by a common cathode. Each TPC consists of three parallel wire planes: the first, facing the drift region, with horizontal wires (Induction plane); the other two with the wires at $\pm 60^\circ$ from the horizontal direction (Induction and Collection planes, respectively). The wire pitch is 3 mm. The maximum drift path, i.e. the distance between the cathode and the wire planes, is 1.5 m and the nominal drift field 500 V/cm (a 3 m drift is foreseen for future ICARUS modules).

Each signal wire of the chamber is independently digitized every 400 ns. The electronics was designed to allow continuous read-out, digitization and independent waveform recording of signals from each wire of the TPC. The measurement of the T_0 time of the event together with the electron drift velocity information, provides the absolute position of the tracks along the drift coordinate.

A fundamental requirement for the performance of the liquid argon TPC is that electrons produced by ionizing particles can travel "unperturbed" from the point of production to the collecting planes. To this end impurities in the liquid must be reduced to a very low level. In order to ensure stable performance of the device, the purity must be preserved in the dewar hosting the inner detector for the longest possible period of time.

The major electronegative impurities in liquid argon which are of importance for the TPC are electron attaching oxygen and/or fluorinated or chlorinated compounds. To achieve long electron drift paths the liquid must be free of these impurities, which will otherwise decrease the electron collection efficiency. To reach a negligible attenuation over the full drift distance, the concentration of impurities must be kept at the level of less than 0.1 part per billion (ppb) oxygen equivalent. Standard commercial LAr has a much higher contamination (typically a few parts per million oxygen equivalent); moreover, LAr can be contaminated inside the cryostat from outgassing of the walls and TPC components (electrodes, cables, etc.). The required purity is therefore achieved with the help of a continuous purification of the liquid via the method of recirculation. A considerable amount of R&D has been performed in order to master this purification process [1]. A detailed description of the T600 purification system can be found elsewhere [2].

The level of purity inside the LAr volume is controlled on-line by an array of dedicated devices, called "purity monitors" [2,4]. The purity monitor consists of a small double-gridded drift chamber, immersed in the LAr volume outside the imaging region. Bunches of electrons are extracted from the cathode via photo-electric effect by means of UV light spots generated by a Xe lamp, transported onto the photo-cathode by a quartz fiber. During the electron drift (16 cm distance), attachment to impurities may take place reducing the amount of charge collected by the anode compared to the charge extracted. The ratio of these charges is a function of the drift electron lifetime in LAr, that can therefore be estimated. The lifetime is directly related to the impurity concentration by an inverse linear relationship. The lifetime estimation thus provides a direct measurement of the LAr impurity content.

Another method based on the off-line analysis of long minimum ionizing tracks traversing a large fraction of the drift space between the cathode and the anode planes, was applied for an independent lifetime estimation and is reported in this paper. This method is of major interest since the detailed imaging of the tracks allows to directly observe the exponential attenuation of the collected charge as a function of the drift time. This information is richer than the simple ratio obtained with the purity monitors.

The comparison between the drift electron lifetimes measured by the purity monitors and with the minimum ionizing tracks is also relevant since these measurements are done at different electric fields: 0.05–0.15 kV/cm for the purity monitors and 0.3–1 kV/cm for the tracks. In Section 6, we show that these measurements are consistent among them. This implies that over the adopted electric field values, the dependence of the electron attachment cross-section is weak. These measurements can therefore be interpreted as direct probes of the remnant impurities in the liquid.

The first T600 half-module was fully instrumented during the year 2000, including the electrical connections and cabling to the outside electronics and DAQ. After assembly, the detector was activated for a technical run that took place on surface in Pavia (Italy) during summer 2001 and which lasted about 3 months. During this period the detector performance was extensively studied and more than 25 000 cosmic-ray events were recorded [2].

The paper is organized as follows: the off-line track reconstruction technique and the electronics calibration are described in Sections 2 and 3, respectively. The results on the determination of the electron drift velocity as a function of the electric field are given in Section 4. Finally, Sections 5 and 6 are devoted to the LAr purity measurements and their interpretation in terms of the detector performance.

2. Event reconstruction

When an ionizing event occurs in the detector active volume the DAQ system continuously stores the charge information (signal waveform) collected by each wire during the drift of electrons. In Fig. 2 we show, as an example, the complete view of one event with multiple parallel tracks (presumably muons) recorded with the T600 detector. The display corresponds to the projection of the event given by the collection view of the left chamber, and has been split in two (top and bottom) pictures. The horizontal axis corresponds to the wire coordinate (17 m total length) with the wire pitch of 3 mm and the vertical to the drift coordinate (1.5 m) sampled every 400 ns. The gray level of the pixels represents the pulse height, proportional to the collected charge. Tens of long parallel minimum ionizing tracks (dark thin lines over light gray background) traveling across the drift volume can be easily identified. The length of these tracks in space is about 2.5 m.

The goal of the reconstruction procedure is to extract the charge deposited by the particle along the ionization track and the point where such a deposition occurred, in order to build a complete spatial and calorimetric picture of the event. The basic building block of a track (called "hit") corresponds to the segment whose ionization charge is read by a single wire of the readout planes. The hits are automatically reconstructed in each wire by a suitable algorithm.

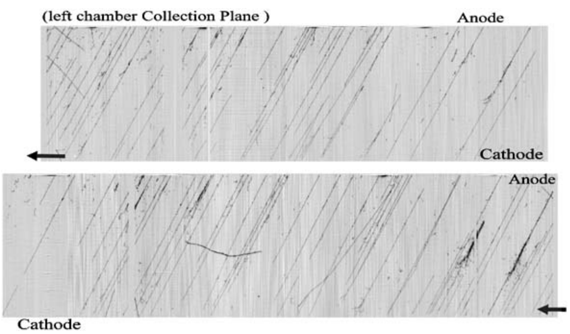

Fig. 2. Event with multiple parallel tracks (collection view on the left chamber) recorded with the T600 detector. The display of the event has been vertically split in two parts of 8 m (top) and 9 m (bottom) length, respectively. The wire coordinate is shown on the horizontal axis, whereas the overall drift time (vertical axis) corresponds to 1.5 m of drift distance.

The waveform of a signal recorded on a wire of the collection plane for the event shown in Fig. 2 is reported in Fig. 3. On the top plot, showing the full time spectrum (4096 time samples of 400 ns each), up to four hits from different muon tracks can be clearly identified above the baseline.

The extraction of the physical parameters from the waveforms can be performed by using analytical functions. The expression used to fit the collection view waveforms is the following function of the drift time (t):

$$F_{\mathrm{c}}(t) = B + A\,\frac{\mathrm{e}^{-(t-t_0)/\tau}}{1+\mathrm{e}^{-(t-t_0)/R_{\mathrm{t}}}} \tag{1}$$

where A is proportional to the peak pulse height, t_0 is the signal peak time, R_{t} and τ are the signal rise and decay times, respectively, and B the baseline. Expression (1) is quite flexible and able to reproduce different data by means of five parameters. The bottom plot of Fig. 3 shows a zoom and the result of the fit in the region surrounding the first hit. Despite the fluctuations of the

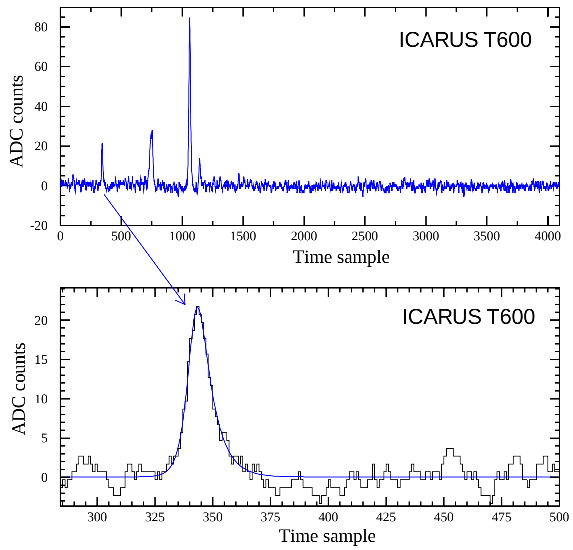

Fig. 3. Example of a collection view signal waveform. Full drift time (top) and zoom in a time window around the first hit maximum (bottom). The continuous line shows the result of the fit with the function given in Eq. (1). A time sample corresponds to 400 ns.

waveform determined by the electronic noise, the signal pulse is well reproduced by the fit.

Because of a fast signal shaping (*RC* few μs), the hit amplitude (units of [ADC×sampling time]) is obtained by numerical integration of the fitted signal function above the baseline. The charge ΔQ (expressed in fC) is obtained by conversion of the hit amplitude with the appropriate calibration factor extracted from the test-pulse calibration of the electronic chain (see Section 3). The hit position is also computed on the induction views to be used in the spatial reconstruction.

The event spatial reconstruction of each individual track consists of (1) a pattern recognition stage, based on the search for a set of aligned points amongst the hits selected by the hit finding algorithm, and (2) of a linear fit procedure through the hits, to calculate the parameters (slope and intercept) of the track in the three independent two-dimensional frames defined by each of the wire planes. The track direction in space is obtained without ambiguities by combining at least two of the three pairs of parameters. This allows to calculate the track angle with respect to the collection plane where the deposited charge is measured. The *effective track pitch length* (Δz) in space (effective portion of the track exposed to the wire) is then given by

$$\Delta z = \frac{\delta}{\cos \gamma} \tag{2}$$

where $\delta = 0.3$ cm is the wire pitch and γ is the angle formed by the track direction and the direction of the collection wire pitch.

Once the track is reconstructed the electron drift velocity can be measured by using tracks crossing both the cathode and the wire planes of the chamber (see Section 4). The LAr purity level, expressed in terms of electron drift lifetime can also be estimated from the attenuation of the collected hit amplitude with the distance, as shown in Section 5.

3. Calibration of the read-out electronics

The T600 electronic chain is composed of three basic units [4]:

(1) the *decoupling board*, which receives analogue signals from the TPC wires and passes them to the *analog board*;
(2) the *analog board*, which houses the signal amplifiers and provides the data conversion at 40 MHz rate for 16 multiplexed channels (each corresponding to a single wire);
(3) the *digital board*, with the circular digital buffers and the VME interface.

Three sets of calibration capacitances were installed along the read-out electronic chain in order to verify the linearity and to calibrate the system: the first, placed on the analog board before the front-end pre-amplifier (3% RMS error on the nominal capacitance value); the second, positioned on the decoupling board (3% RMS error); the third, mounted on the far end of the read-out wire, immersed in LAr. The use of different test capacitances allows to disentangle various systematic effects possibly due to fluctuations in the value of the test capacitances themselves.

The test pulses used to perform the calibration of the read-out chain had a step function shape. The values of the injected charge (ranging from 3 to 90 fC) allow a check of the electronics linearity from 1 to about 30 m.i.p. equivalent charge deposition. The test pulse waveforms were analyzed by using the standard hit finding algorithm for ionizing tracks, each waveform signal being fitted with Eq. (1) and the hit amplitude calculated.

As an example, Fig. 4 shows the measured charge for a 23 fC test pulse injected on the decoupling boards of the 5728 collection wires, together with the distribution of measured hit amplitudes on all wires fitted with a Gaussian (inset of Fig. 4). The observed RMS is consistent with the expected value from the intrinsic spread of the test capacitances. Similar compatible results were obtained using test pulses injected on the analog boards.

The linear behavior of the global calibration curve using the analog board test data is presented in Fig. 5. The mean value of the Gaussian fits is plotted as a function of the injected charge. The straight line fit provides the calibration factor, $(152 \pm 2) \times 10^{-4}$ fC/[ADC×sampling time] (error

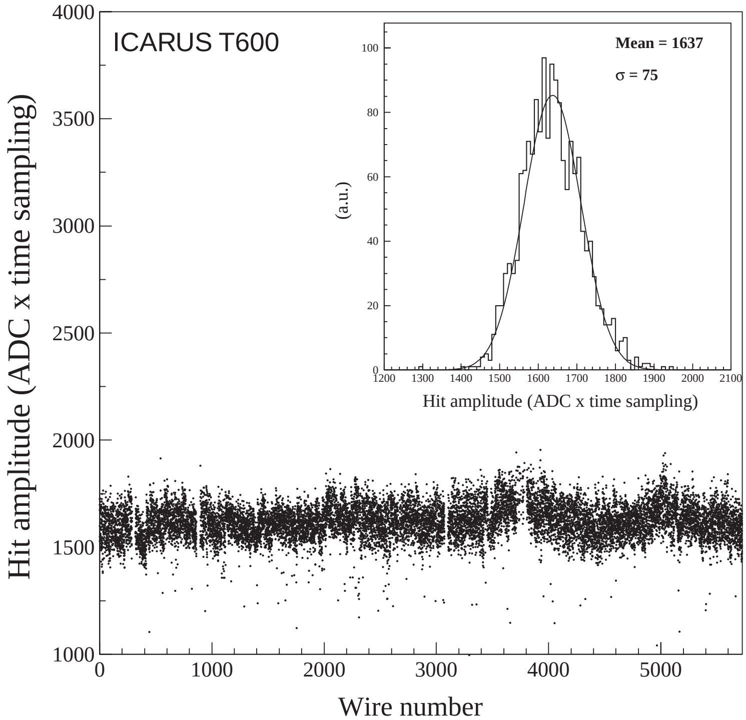

Fig. 4. Distribution of the hit amplitudes (400 ns of sampling time) measured on each collection wire for a 23 fC test pulse injected on the decoupling boards. The distribution of the hit amplitudes on all wires, fitted with a Gaussian function, is also shown (inset).

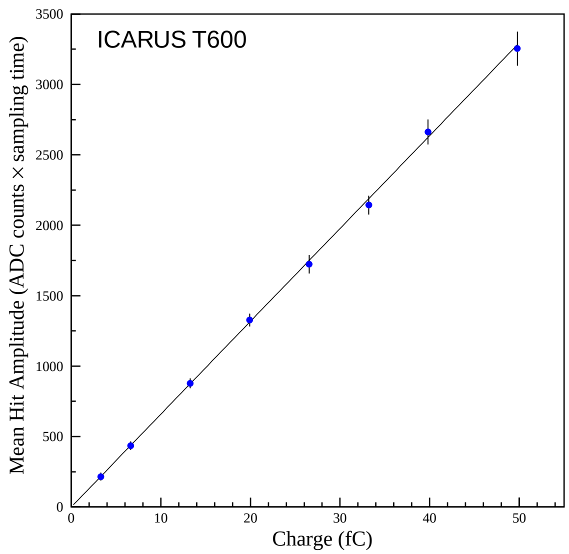

Fig. 5. Linearity of the electronics (analog board data): mean value of the Gaussian fit as a function of the injected charge (from 1 to about 30 m.i.p. equivalent). The calibration factor, $(152 \pm 2) \times 10^{-4}$ fC/[ADC× sampling time], is given by the inverse of the slope.

from the fit), and demonstrates the linearity of the read-out chain over a wide range of deposited charge. The individual wire-to-wire fluctuations of the calibration factor follow the spread on the nominal value of the capacitances ($\pm 3\%$).

4. Measurement of the electron drift velocity

The electrons released by ionizing particles crossing the LAr volume are transported towards the anode planes with an electric field-dependent *drift velocity* v_{d}. The knowledge of the drift velocity is necessary to reconstruct the track coordinate along the drift direction.

The electron drift velocity depends not only on the value of the electric field but also on the LAr temperature. The stable LAr temperature conditions obtained during the T600 technical run (maximum $\Delta T \leqslant 1$ K [2,5]) allow to outline the drift velocity behavior as a function of the electric field without local distortions.

Three different samples of data were used for the v_d measurements: (1) single, long minimum ionizing tracks crossing the volume from anode to cathode or vice versa, (2) large shower events extending over the whole drift region, and (3) signals from the purity monitors. In all three cases the drift velocity was extracted from the ratio of the cathode–anode distance and the measured electron drift time: $v_d = l_{CA}/t_{CA}$.

For the two first data samples (single tracks and showers) l_{CA} is the maximum drift distance for cooled detector conditions (1482 mm). The drift time t_{CA} is obtained using the recorded signal waveforms from the two wires corresponding to the entry point and to the exit point of the tracks. In the purity monitor sample, l_{CA} is the distance between the anode and cathode grids (160 mm) and t_{CA} is the measured drift time of the electron bunch between the two grids.

The measured values of the electron drift velocity from the three data samples at different electric fields ($|\vec{E}|$) are reported in Table 1. These values corrected for temperature are consistent with data previously measured by using smaller detector prototypes [6,7]. For the minimum ionizing tracks and shower events, the error on the determination of the drift velocity due to the dispersion of the measurements includes (1) the precision on the knowledge of the cathode–anode distance, that can locally vary because of the non-perfect planarity of the cathode (less than 5 mm), and (2) by the small gradients of temperature inside the LAr volume.

The compilation of the results for drift velocities at low (purity monitors) and high electric fields is presented in Fig. 6 (points) together with the result of a 5-parameter polynomial fit to the data (solid line). The polynomial function describes very well the behavior of v_d over the whole range of electric fields. For comparison, the prediction from the empirical function proposed in Ref. [8], calculated at the nominal temperature of 89 K, is also shown (dashed line). The two results are in good agreement.

Table 1
Measured values of the drift velocity (v_d) for different electric field strengths ($|\vec{E}|$) at $T = 89$ K from physical events and purity monitor data samples

$\|\vec{E}\|$ (kV/cm)	v_d (mm/μs)	Event type
Imaging sample		
0.304	1.169 ± 0.003	Tracks
0.405	1.385 ± 0.005	Tracks
0.506	1.551 ± 0.015	Tracks
	1.56 ± 0.02	Shower
0.607	1.682 ± 0.012	Tracks
	1.68 ± 0.02	Shower
0.708	1.792 ± 0.025	Tracks
	1.78 ± 0.03	Shower
0.810	1.893 ± 0.025	Tracks
0.911	1.964 ± 0.006	Tracks
1.012	2.057 ± 0.011	Tracks
	2.03 ± 0.03	Shower
Purity monitor sample		
0.056	0.289 ± 0.002	
0.075	0.381 ± 0.006	
0.1	0.499 ± 0.010	
0.15	0.694 ± 0.008	

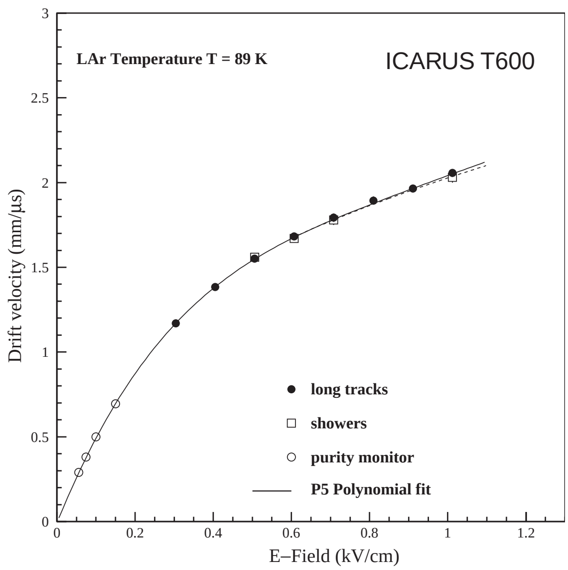

Fig. 6. Electron drift velocity in LAr as a function of the electric field, as measured in the ICARUS T600 half-module. Data from purity monitor measurements (open circles), from crossing single muon tracks (full circles) and from shower data (squares). The result of the P5-polynomial fit through all points (solid line) together with the analytical prediction from Ref. [8] assuming $T = 89$ K (dashed line) are also shown.

5. Drift electron lifetime and LAr purity

Argon purification is performed by means of a liquid and a gas recirculation systems. On top of the detector, the recirculation of the gas phase is implemented by flowing the gas through commercial purification cartridges.[1] The recirculation in liquid phase is performed by a pump which forces liquid argon into similar commercial cartridges.

The main purpose of the liquid recirculation unit is to purify the bulk LAr volume until the purity level for efficient operation is reached. The gas recirculation unit prevents impurities coming from potential leaks on top of the container (from flanges or feedthroughs) or from outgassing of the "hot" portions of the detector (e.g. readout cables inside the chamber but not immersed in the LAr, etc.) to diffuse into the liquid volume.

In the next subsections, we describe the two methods used to measure the drift electron lifetime. The method described in Section 5.1 is based on the use of the purity monitors that provide an on-line and local estimate of the drift electron lifetime. The second method, treated in Section 5.2, is based on the off-line analysis of the collected events, by studying the attenuation of the signal amplitude as a function of the electron drift distance.

5.1. Measurements with the purity monitors

The purity monitor geometry and the applied electric field are such that the method is sensitive up to several milliseconds lifetime with errors at the level of $<10\%$ [2]. The purity monitors were positioned at different heights in order to follow the drift electron lifetime level during the filling of the cryostat, to provide redundant readings during the steady-running phase, as well as indications on any possible lifetime gradient in the volume.

The drift electron lifetime evolution measured by the purity monitor located close to the extraction point of the LAr recirculation system (in one corner of the volume, at about 3.6 m height from the bottom of the cryostat) is reported in Fig. 7 (*dots*). The first data points indicated a value in the range of 250 μs. The electron lifetime increased steadily when the recirculation systems were operated. At the run stop, the lifetime reached a maximum value of about 1.8 ms ($\pm 8\%$ error) and was still growing. The trend in Fig. 7 clearly shows how the steady increase of the drift electron lifetime was interrupted during the period when the liquid recirculation was turned off. Running in absence of liquid recirculation allowed us to directly estimate the amount of impurities diffusing into the liquid argon volume (see Section 6).

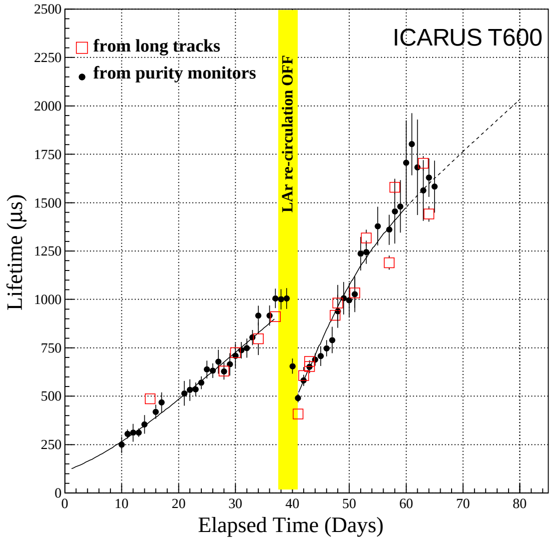

Fig. 7. Evolution of the free electron lifetime during the T600 test run from purity monitor (*dots*) and from ionizing tracks analysis (*squares*). The period when the liquid re-circulation was switched off is indicated. The solid line shows the fit result (Eq. (4)). See text for more details.

5.2. Measurement from minimum ionizing tracks

This method can be summarized as follows: after the spatial reconstruction of the track, we consider the distribution of the charge measured on the collection wires (ΔQ) for 15 slices of the drift coordinate (10 cm wide each). For each slice, the value of the most probable charge released by the track (ΔQ_{mp}) is extracted by fitting the distribution to a Landau function, convoluted with a Gaussian function that describes the effect of the electronic noise of the read-out system.

[1] Oxysorb and Hydrosorb from Messer-Griesheim.

ΔQ_{mp} corresponds to the most probable value of the fitted distribution. Once this procedure is applied to all slices, the electron lifetime is given by an exponential fit of ΔQ_{mp} as a function of the drift coordinate.

Fig. 8 shows the result of such a fit obtained for selected tracks of the event shown in Fig. 2. The inverse of the slope gives a drift electron mean free path of 220 cm corresponding to a drift electron lifetime of 1.43 ± 0.07 ms (error from the fit). This value can be considered as the *average* electron lifetime within the chamber, since the chosen tracks span the full liquid argon volume in a rather uniform way. The quoted error is dominated by the statistical error on the determination of the most probable value for each slice.

The measured value of the electron lifetime τ_e can be used to account for the charge attenuation occurring during the drift process and to reconstruct the "corrected charge" ΔQ_{cor} released by the track:

$$\Delta Q_{cor} = e^{t_d/\tau_e} \Delta Q \tag{3}$$

where ΔQ is the charge measured on the wire and t_d is the drift time associated to the hit, obtained from the peak time of the hit and the T_0 of the

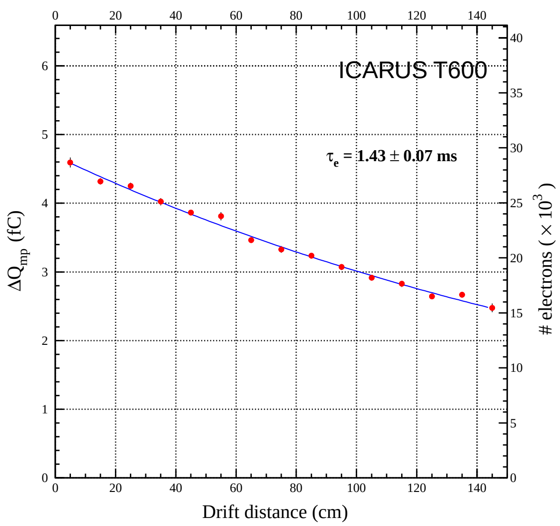

Fig. 8. Determination of the drift electron lifetime from minimum ionizing tracks crossing the detector (event in Fig. 2): exponential fit of the most probable value of the measured charge as a function of the drift distance (15 slices). The number of equivalent electrons is indicated on the right vertical axis.

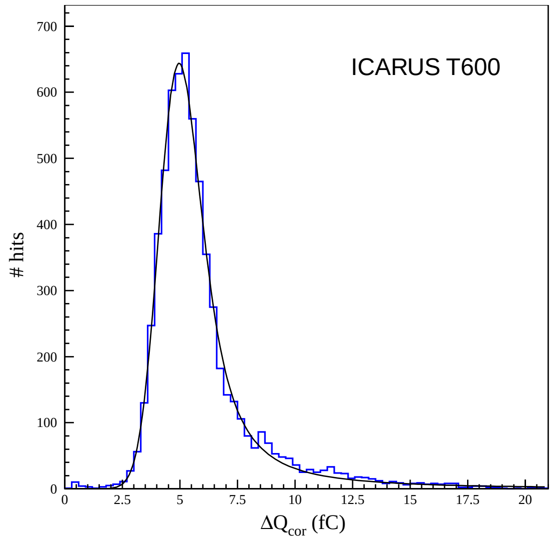

Fig. 9. Overall distribution of the charge released by the crossing tracks of the event shown in Fig. 2 after electron lifetime correction.

event. The overall distribution of ΔQ_{cor} from the tracks of the event shown in Fig. 2 is reported in Fig. 9, together with the result of a fit to a Landau convoluted with a Gaussian function (solid line). The value of the most probable corrected charge released (ΔQ_{mp}) corresponds to 4.70 ± 0.03 fC, equivalent to about 29 300 electrons, for an effective track pitch length of $\Delta z \simeq 0.61$ cm.

The same procedure was used to extract the electron lifetime at different data periods. The summary of the obtained values of τ_e as function of time is reported in Fig. 7 (squares).

6. Interpretation of the electron drift lifetime data

As shown in Fig. 7, there is a rather good consistency between the purity monitor measurements and the values of the electron lifetime obtained using long minimum ionizing tracks. The measurements performed with data from cosmic rays confirm the evolution of the LAr purity level as observed with the purity monitor. Moreover, this measurement demonstrates a good uniformity of the LAr purity over the whole volume within the measurement precision, being the tracks randomly distributed in the liquid argon volume unlike the purity monitor which gives a punctual measurement.

The concentration of impurities in the LAr volume, N, is determined by (a) the purification process and (b) the continuous input of impurities, both functions of time. The differential equation that describes the time-evolution of N can be written as

$$\frac{\mathrm{d}N}{\mathrm{d}t} = -\Phi_{\mathrm{out}}(t) + \Phi_{\mathrm{in}}(t) = -\frac{N(t)}{\tau_{\mathrm{c}}} + \Phi^0_{\mathrm{in}} + \frac{A}{(1+t/t_0)^B} \quad (4)$$

where the first term takes into account the purification process, with a characteristic purification time τ_{c} given by the time needed to circulate the whole LAr volume (about 4.5 days for the T600 half-module). The second term Φ^0_{in} represents a constant input rate of impurities. Finally, the outgassing of material in contact with the argon is taken into account by the third term with a time power-law. The t_0 time is fixed relative to the time at which the dewar started to be cooled, while A (normalization factor) and B (that governs the outgassing speed) are extracted from the fit of the data to Eq. (4).

Asymptotically, the best possible reachable level of purity is given by the equilibrium between the input of impurities and the purification speed. This value is determined by the product of the recirculation time and the constant input of impurities, $\Phi^0_{\mathrm{in}}\tau_{\mathrm{c}}$, since the outgassing, dominant source of impurities at the beginning, tends to zero for infinite time.

The result of the fit of the purity monitor data with Eq. (4) (solid line in Fig. 7) gives a constant input factor compatible with zero, $\Phi^0_{\mathrm{in}} = (5 \pm 5) \times 10^{-3}$ ppb/day oxygen equivalent. The fitted values for the outgassing parameters are $A = 0.33 \pm 0.07$ ppb/day and $B = 1.39 \pm 0.05$. Hence, we conclude that there is an indication for a time-dependent contribution, typical of an outgassing process. Given the experimental sensitivity, the constant input rate is consistent with zero. Accordingly, the results are consistent with the assumption that the dominant source of outgassing is located in the "hot" parts of the detector (e.g. readout cables outside the liquid, etc.) and no significant time-independent contribution (leak, etc.) that would limit the asymptotic purity level. Under these assumptions, one can extrapolate the fit to infinite time to find an asymptotic drift electron lifetime $\gtrsim 13$ ms (dashed line in Fig. 7). This result makes us confident about the understanding and the control of the liquid argon purity.

7. Conclusions

In this paper we have reported measurements concerning the liquid argon purity achieved with the first half-module of the ICARUS T600 detector. The data were recorded in a technical run that took place at surface with cosmic rays.

Results from the electronics calibration using test pulse events on test capacitances at different voltages have been presented. A linear behavior over a charge range from 1 to about 30 m.i.p. equivalent is observed.

A detailed study of the free electron drift velocity dependence on the electric field has been performed. Three different types of data (from purity monitors, from single muon tracks and from shower events) were used to cover low (0.056–0.150 kV/cm) and high (0.3–1 kV/cm) electric field domains. The results presented here are in good agreement with earlier published measurements.

Two independent and complementary techniques were used to measure the evolution of the LAr purity during the run. The first one, based on dedicated devices called purity monitors, provided on-line values of the drift electron lifetime at localized points inside the LAr volume. The second method uses long minimum ionizing tracks and is based on the study of the attenuation of the signal amplitude with the drift distance. Both methods show consistent results over the whole data taking period. Since the selected tracks were randomly distributed over the volume, the compatibility between the purity monitor and the tracks is consistent with a uniform purity within the whole volume.

Since the measurements performed with the purity monitors and the tracks occurred at different electric fields, the comparison between the drift electron lifetime obtained with the two methods is a test of the dependence of the electron attachment cross-section on the electric field. We find that in the range 0.05–1 kV/cm, the dependence of the attachment cross-section is weak. This measurement is therefore a direct probe of the remnant impurities in the liquid.

At the end of the run the drift electron lifetime reached a maximum value of about 1.8 ms, equivalent to an electron mean free path longer than 280 cm, and was still increasing. These results are consistent with a vanishing leak rate (smaller than 0.01 ppb/day). It appears that the drift electron lifetime was not limited by the low observed constant leak of impurities but only by the total duration of the test run. These results give us confidence that the drift distances in future ICARUS modules could be expanded to at least 3 m with no major modifications of the present technology.

Acknowledgements

We would like to warmly thank the many technical collaborators that contributed to the construction of the detector and to its operation. In particular we acknowledge the precious contribution of the LNGS mechanical workshop during the design and realization purity monitor system. We are glad of the financial and technical support of our funding agencies and in particular of the Istituto Nazionale di Fisica Nucleare (INFN), of ETH Zürich and of the Fonds National Suisse de la Recherche Scientifique, Switzerland. The Polish groups acknowledge the support of the State Committee for Scientific Research in Poland, 2P03B09520, 2P03B13622, 160/E-340/SPB/ICARUS/P-03/DZ212/2003-2005, 620/E-77/SPB/ICARUS/P-03/DZ213/2003-2005, 621/E-78/SPB/ICARUS/P-03/DZ214/2003-2005, 105/E-344/SPB/ICARUS/P-03/DZ211/2003-2005; the INFN, FAI program; the EU Commission, TARI-HPRI-CT-2001-00149. The Spanish group is supported by the Ministry of Science and Technology (project FPA2002-01835).

References

[1] ICARUS Collaboration, A second-generation proton decay experiment and neutrino observatory at the Gran Sasso Laboratory, LNGS-94/99-I (1994) and references therein.
[2] ICARUS Collaboration, The ICARUS T600 detector, in preparation.
[3] F. Arneodo, et al., (ICARUS Collaboration), Nucl. Instr. and Meth. A 432 (1999) 240.
[4] F. Arneodo, et al., (ICARUS Collaboration), A second-generation proton decay experiment and neutrino observatory at the Gran Sasso Laboratory, LNGS-EXP 13/89 add.2/01 and references therein.
[5] J. Rico, Ph.D. Dissertation ETH 14906, 2002. Available at: http://neutrino.ethz.ch/diplomathesis.html.
[6] P. Cennini, et al., Nucl. Instr. and Meth. A 345 (1994) 230.
[7] F. Arneodo, et al., (ICARUS Collaboration), Nucl. Instr. and Meth. A 498 (2003) 292.
[8] W. Walkowiak, Nucl. Instr. and Meth. A 449 (2000) 288.